Photodiagnosis and Photodynamic Therapy 26 (2019) 244–251

Contents lists available at ScienceDirect

Photodiagnosis and Photodynamic Therapy

journal homepage: www.elsevier.com/locate/pdpdt

Curcumin-mediated photodynamic inactivation (PDI) against DH5α contaminated in oysters and cellular toxicological evaluation of PDI-treated oysters

Yuan Gao[a], Juan Wu[a,b], Zhaojie Li[a], Xu Zhang[a], Na Lu[a], Changhu Xue[a], Albert Wingnang Leung[c], Chuanshan Xu[d,**], Qingjuan Tang[a,*]

[a] Laboratory of Food Science and Human Health, College of Food Science and Engineering, Ocean University of China, Qingdao, China
[b] Innovation Center for Marine Drug Screening and Evaluation, Marine Biomedical Research Institute of Qingdao, 266071, China
[c] School of Chinese Medicine, Faculty of Medicine, The Chinese University of Hong Kong, Shatin, Hong Kong, China
[d] Key Laboratory of Molecular Target and Clinical Pharmacology, State Key Laboratory of Respiratory Disease, School of Pharmaceutical Sciences & Fifth Affiliated Hospital, Guangzhou Medical University, Guangzhou, China

ARTICLE INFO

Keywords:
Oysters
Curcumin-mediated photodynamic inactivation
DH5α cells
Reactive oxygen species
Membrane permeability
Cellular toxicology
Antimicrobial Photodynamic Therapy

ABSTRACT

The objective of this study was to evaluate the bactericidal effect of curcumin (CUR)-mediated photodynamic inactivation (PDI) against *Escherichia coli* DH5α *in vitro* and in oysters, then further investigate the edible security of PDI-treated oysters based on cellular toxicological methods. First, DH5α cells were irradiated by a 470 nm LED light source with an energy density of 3.6 J/cm^2. Colony forming units (CFU) were counted and the viability of DH5α cells was calculated after treatment with CUR-mediated PDI. Intracellular production of reactive oxygen species (ROS) was studied by measuring the fluorescence of 2, 7-dichlorofluorescein (DCF) using a flow cytometry. Membrane permeability was measured using confocal laser scanning microscopy (CLSM) with propidium iodide (PI) staining. After that, the bactericidal effect of CUR-mediated PDI was evaluated in oysters which were pre-contaminated with DH5α cells. Finally, cellular toxicology of PDI-treated oysters was evaluated through morphological observation, 3-(4, 5-dimethylthiazol-2-yl)-2, 5-diphenyltetrazolium bromide (MTT) assay, DNA ladder assay, and nuclear staining. Results showed that the viability of DH5α was significantly decreased in a CUR concentration-dependent manner and resulted in an approximately 3.5-log reduction at the concentration of 20 μM. After treatment with CUR-mediated PDI (20 μM, 3.6 J/cm^2), the ROS level in DH5α cells and the membrane permeability markedly increased. Our data demonstrated that CUR-mediated PDI had a good decontamination effect against DH5α contaminated in oysters. After incubation with PDI-treated oysters, fibroblasts L929 cell morphology, MTT absorbance and cell apoptosis had no obvious changes. Our findings preliminarily demonstrated that CUR-mediated PDI-treated oysters had no cytotoxicity to fibroblasts.

1. Introduction

Concern about seafood safety has increased as seafood contaminated with pathogenic microorganism can threaten consumer's daily life by causing serious illnesses [1]. Foodborne outbreaks derived from consuming raw or under-cooked seafood are major causes of illness. Bivalves like oysters are filter feeders that ingest food particles from seawater through gills, which may contain infectious agents. Gills and labial palps select and direct food to the mouth, then going to the stomach to be digested, and finally, reaching digestive tubules to absorption; undigested materials go to intestine [2]. Oyster is one of the most common seafood containing abundant nutrients and active ingredients. However, its nonselective filter-feeding character causes a large variety of pathogenic microorganisms enriched in its body [3]. The current potential strategies for decontaminating shellfish include heat treatment [4], chlorine-based sanitizers [5], irradiation [6] and high pressure processing (HPP) [7]. However, these treatments have some drawbacks [8–10]. Therefore, it is an urgent need to find some cold-sterilization technologies with broad-spectrum antibacterial features for the raw seafood consumption. More importantly than that, it

* Corresponding author at: College of Food Science and Engineering, Ocean University of China, No 5, Yushan Road, Qingdao, Shandong Province, 266003, China.
** Corresponding author at: Key Laboratory of Molecular Target and Clinical Pharmacology, State Key Laboratory of Respiratory Disease, School of Pharmaceutical Sciences & Fifth Affiliated Hospital, Guangzhou Medical University, Guangzhou, Guangdong Province, 511436, China.
E-mail addresses: xcshan@163.com (C. Xu), tangqingjuan@ouc.edu.cn (Q. Tang).

https://doi.org/10.1016/j.pdpdt.2019.04.002
Received 3 January 2019; Received in revised form 1 March 2019; Accepted 1 April 2019
Available online 03 April 2019
1572-1000/

must effectively eliminate or reduce microbial contamination *in vivo* and be environmentally friendly without compromising on the quality of seafood and public health.

Photodynamic inactivation (PDI) of microorganisms has been considered as a promising method [11,12] with an efficient inactivation against multi-resistant bacteria and fungi [13,14]. It combines a non-toxic photosensitizer (PS) with visible light in the presence of oxygen to kill the microbial cells [15], and involves delivering visible light of the appropriate wavelength to excite the PS to produce reactive oxygen species (ROS) such as superoxide, hydroxyl radicals and singlet oxygen [16]. So far, PDI has proved to be efficient against viruses [17], bacteria [13,17], fungi [18] and parasites [19], without the risk of adverse effects to the normal cells.

In the process of PDI, PS plays a crucial role in generating ROS [20], which can cause significant oxidative damage to the microbial cells. Thus, development of a PS with better efficacy, more safety and greater producing ROS potential is vital importance [21]. Traditional Chinese medicine (TCM) represent a rich resource for identifying potential novel PSs [22]. Curcumin (CUR), isolated from the rhizomes of TCM *Curcuma longa*, is a naturally occurring polyphenolic compound [23]. It has been used as a medicine, spice and a food additive in China and elsewhere [24,25] for its diverse biological activities [26–30]. Reports showed that 400–500 nm visible light irradiation could activate curcumin and produce ROS to kill microorganisms [3,31–33]. According to our recent studies, curcumin-mediated PDI could effectively inactivate murine norovirus and *Vibrio parahaemolyticus* which were contaminated in oysters and the working conditions of curcumin-mediated PDI on oysters have been optimized [3,34].

In the present study, we extended our studies and chosen *Escherichia coli* DH5α as an example to evaluate the viability of DH5α following curcumin-mediated PDI *in vitro* and in oysters. Finally, the edible security of PDI-treated oysters was preliminarily investigated based on cellular toxicological methods.

2. Materials and methods

2.1. Bacteria and cell culture

Bacterial strain DH5α used in the study was purchased from National Collection of Type Cultures (Public Health England, Porton Down, Salisbury, UK). After growing overnight at 37 °C in Luria-Bertani (LB) Broth (Beijing Land Bridge Technology Company Ltd., Beijing, China), the bacteria were shaked for 3 h at 37 °C in LB broth medium. Bacterial suspension was centrifuged at 4500 rpm for 15 min at room temperature, the supernatant discarded and the cell pellet was re-suspended in sterile PBS buffer (pH 7.4) to a final concentration of 10^8 CFU/ml.

Fibroblasts L929 cell lines (ATCC, Rockville, MD, USA) was cultured in DMEM medium supplemented with 10% new born calf serum (NBCS) and antibiotics (penicillin 100 U/mL and streptomycin 100 lg/mL; Invitrogen Co., Carlsbad, CA, USA). Cells were maintained at 37 °C in a water-saturated atmosphere with 5% CO_2 / 95% air.

2.2. Photosensitizer (PS) and light source

Curcumin solution was prepared as previous reports [3,31]. Stock solution of curcumin (95% purity) (Ci Yuan Biotechnology Co., Ltd. Shanxi, China) was dissolved in edible alcohol (Food Grade, 95% ethanol; Tianjin Guayue Group Co., Ltd. Tianjin, China) with the concentration of 40 mM and kept in the dark at −20 °C until use. The working solution was diluted with artificial seawater (salinity 3.3%) in the artificial seawater system to the concentrations of 5 μM, 10 μM and 20 μM.

Light irradiation was delivered using a light-emitting diode (LED) blue light source which was supplied by School of Chinese Medicine, the Chinese University of Hong Kong. The samples were exposed to LED light (wavelength of 470 nm, energy density of 3.6 J/cm^2: optical power density was fixed at 0.06 W/cm^2 with an irradiation time of 60 s) as our previous reports [35–37].

2.3. Photodynamic treatment on DH5α cells

Working cultures of DH5α (10^8 CFU/ml) were incubated with a range of concentrations of curcumin (5, 10, 20 μM) in 6-well plates in the dark at 37 °C for 5 min [34]. Then the bacterial suspension was irradiated by the LED light source at the energy density of 3.6 J/cm^2. After light irradiation, bacteria cells were serially diluted 10-fold in sterile PBS buffer. Each sample (1 ml) was spread on LB agar (Beijing Land Bridge Technology Company Ltd., Beijing, China) plates and incubated for 24 h at 37 °C in the dark. The colony forming units (CFU) were counted and the viability of bacteria was a log value of CFU per ml. Each sample was set three parallel tests and the experiment was at least repeated for three times.

The experiment was randomly divided into 4 groups; 1) negative control (no PS, no irradiation, L-S-), 2) CUR treatment alone (20 μM) (with PS, no irradiation, L-S+), 3) LED irradiation alone (no PS, same irradiation as PDI samples, L+S-), and 4) CUR-mediated PDI (5, 10, 20 μM and energy density of 3.6 J/cm^2) (L+S+) as our previous reports [3,36,37].

2.4. Intracellular ROS evaluation

Intracellular ROS production was studied by measuring the fluorescence of 2, 7-dichlorofluorescein (DCF) [38]. The bacterial cells were incubated with CUR (20 μM) in sterile PBS buffer for 5 min and then incubated with 2, 7-dichlorodihydrofluorescein diacetate (DCFH-DA, 10 μM, Beyotime, Jiangshu, China) for 20 min at 37 °C in the dark. After washed with PBS, the bacterial cells were irradiated at the energy density of 3.6 J/cm^2. To examine the yield of intracellular ROS, bacterial cells were harvested and analyzed by flow cytometry (FCM) (Guava PCA, Millipore, USA) after 10 min incubation at 37 °C in the dark. Data were analyzed using the software FCS Express V3 (De Novo Software, Los Angeles, CA, USA).

2.5. Bacterial membrane permeability detection

After treatment with CUR-mediated PDI (20 μM, 3.6 J/cm^2), the bacterial cells were harvested by centrifugation at 10,000 ×g, for 20 min at 4 °C and washed twice with sterile PBS buffer. Then the bacterial cells were incubated with propidium iodide (PI, 100 μg/ml) for 30 min at 4 °C in the dark. After washed with sterile PBS buffer, the bacterial cells were transferred on the surface of a sterile cover glass slide by pipette and observed immediately using a confocal laser scanning microscopy (CLSM). The images were recorded at the excitation wavelength of 535 nm and emission wavelength of 615 nm [36,37].

2.6. Photodynamic treatment on DH5α cells contaminated in oysters

Six oysters in L+S+ group were contaminated with working cultures of DH5α and incubated with a range of concentrations of curcumin (5, 10, 20 μM) in an artificial seawater system (salinity 3.3%) for 3 h at about 10 °C as described in our previous reports [3,34]. The L-S+ group was contaminated with working cultures of DH5α and incubated with 20 μM curcumin. The oysters in L-S- and L+S- groups were only contaminated with working cultures of DH5α. The oysters in L+S+ and L+S- groups were opened with the bottom shell reserved in sterile conditions and then irradiated at the energy density of 3.6 J/cm^2. Then the oyster flesh in each group was removed completely from the bottom shell and combined in a 50 ml sterile centrifuge tube respectively. After weighed, the oyster flesh in each group was added PBS buffer (m/v, 1:9) and homogenized in ice bath. After that, the bacterial

suspension was filtered and the filtrate was serially diluted 10-fold in PBS buffer. Each sample (1 ml) was spread on LB agar plates and incubated for 24 h at 37 °C in the dark. The colony forming units (CFU) were counted and the viability of bacteria was a log value of CFU per gram oyster flesh. Each sample was set three parallel tests and the experiment was at least repeated for three times.

2.7. Preparation of PDI-treated oysters

Six oysters in L+S+ or L-S+ groups were only incubated with CUR (20 μM) in an artificial seawater system (salinity 3.3%) for 3 h at about 10 °C according to the above descriptions. The oysters in L-S- and L+ S- groups were cultured in the seawater system without treatment. The oysters in L+S+ and L+S- groups were opened with the bottom shell reserved in sterile conditions and irradiated at the energy density of 3.6 J/cm^2. Then the oyster flesh in each group was removed completely from the bottom shell and combined in a 50 ml sterile centrifuge tube respectively. After homogenized in ice bath, the supernates were filtered using 0.22 μm filter (Millipore, Merck KGaA, Darmstadt, Germany) and the filtrates were stored at −20 °C until use.

2.8. Morphological detection of L929 cells

Fibroblasts L929 cells treated with the filtrates of PDI-treated oysters were microscopically examined for morphological changes using an inverted contrast microscope (Nikon Eclipse T500, Japan) after incubated for 24, 48, 72, and 96 h at 200 × magnification.

2.9. Cytotoxicity assay

The 3-(4, 5-dimethylthiazol-2-yl)-2, 5-diphenyltetrazolium bromide (MTT) assay was used for evaluation the cytotoxicity of the PDI-treated oysters on the fibroblasts L929 cells. L929 cells (1 × 10^5 cells/ ml) were seeded in 96-well plates and placed in an incubator at 37 °C for 24 h. The medium was then replaced with the filtrates of PDI-treated oysters. After incubation for 24, 48, 72, 96 h, cell viability was determined using MTT assay [39] and the absorbance at 570 nm was measured using microplate reader (Biotek ELX-800 Absorbance Reader, USA). Three separate experiments were performed.

The relative growth rates (RGR) of the treatment groups were expressed in percentages which were obtained from the control group. The calculating formula was as follows:

$$RGR\ (\%) = At / Ac \times 100$$

At: the absorbance of treatment group at 570 nm; *Ac*: the absorbance of control group at 570 nm

Determination of cytotoxicity was based on the RGR and the corresponding cytotoxicity grades which were shown as Table 1: Grades 0 and 1 are considered to have no cytotoxicity; grade 2 is considered to have slight cytotoxicity; grades 3 and 4 are considered to have moderate cytotoxicity; and grade 5 is considered to have extreme cytotoxicity.

2.10. DNA ladder assay

After incubation for 96 h, the L929 cells were harvested and the genomic DNA was extracted using a TIANamp Genomic DNA Kit (TIANGEN Biotech Company Ltd., Beijing, China). The products were separated by 1% agarose gel electrophoresis, stained with ethidium bromide, and visualized using UV light.

Table 1
Standard for evaluation.

RGR	≥ 100	75~99	50~74	25~49	1~24	0
Grades	0	1	2	3	4	5

2.11. Nuclear staining

L929 cells were seeded in 6-well culture plates containing a glass coverslip-covered 15 mm cutout (MatTek, Ashland, MA). The next day, cells were incubated with filtrates of PDI-treated oysters for 96 h at 37 °C and then stained using Hoechst 33258 (10 μg/ml) for 15 min at 37 °C. The stained cells were washed twice with PBS buffer and then observed immediately under a fluorescence microscope with a filter set of Ex/Em of BP330-380/LP420 nm, and recorded the images by a colorful charge-coupled device camera.

2.12. Statistical analysis

The data were expressed as the mean ± standard deviation (SD). Statistical analysis was performed using SPSS v18.0 software (SPSS, Inc., Chicago, IL, USA). Differences between groups were analyzed by one way analysis of variance (ANOVA). A P-value < 0.05 was considered significant and a P-value < 0.01 was considered extremely significant.

3. Results

3.1. Inactivation of DH5α cells after treatment with CUR-mediated PDI

Curcumin-mediated photodynamic inactivation (CUR-mediated PDI) significantly killed DH5α cells as shown in Fig. 1. The viability of DH5α reduced extremely significant ("**" $P < 0.01$) in L+S+ group compared with L-S- group, and the rate of cell death increased in a CUR concentration-dependent manner and resulted in an approximately 3.5-log reduction at the concentration of 20 μM.

3.2. ROS production in DH5α cells

The production of ROS in DH5α cells was analyzed using FCM with DCFH-DA staining. Results of FCM showed the spectral shift of the fluorescence curves to the right after treatment with CUR-mediated PDI at the CUR concentration of 20 μM and energy density of 3.6 J/cm^2, indicating a significant increase of the ROS level in DH5α cells (Fig. 2).

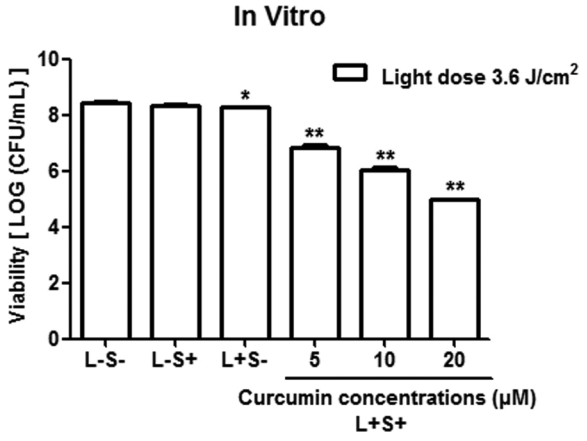

Fig. 1. Viability of DH5α cells.
L-S-: negative control; L-S+: CUR treatment alone (20 μM); L+S-: LED irradiation alone (3.6 J/cm^2); L+S+: CUR-mediated PDI (5, 10, 20 μM and 3.6 J/cm^2). Each column represents the average of triplicates, at least repeated for three times. Values are expressed as mean ± SD. * $P < 0.05$; ** $P < 0.01$, different from the L-S- group.

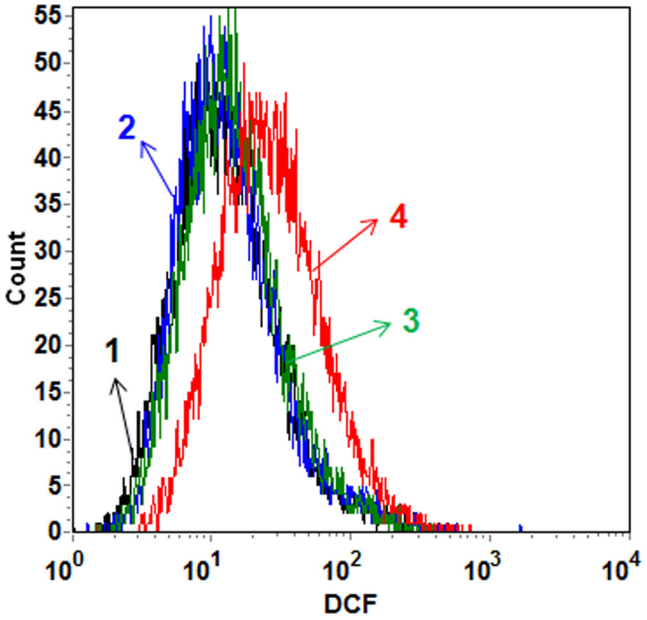

Fig. 2. Intracellular ROS production of DH5α cells.
ROS in DH5α cells was analyzed using FCM with DCFH-DA staining. 1: negative control; 2: CUR treatment alone (20 μM); 3: LED irradiation alone (3.6 J/cm^2); and 4: CUR-mediated PDI (20 μM, 3.6 J/cm^2). It is a representative figure of the final results which were repeated at least for three times.

3.3. Change of bacterial membrane permeability after treatment with CUR-mediated PDI

Membrane integrity is an important factor affecting bacterial survival. PI is a common indicator of cell membrane permeability because PI as a fluorescent nucleic acid binding dyes is usually excluded by the intact cell membranes of bacteria [40]. CLSM with PI staining was used in the present study to explore membrane permeability of DH5α after treatment with CUR-mediated PDI. As shown in Fig. 3, more red fluorescence was found in DH5α cells treated by CUR-mediated PDI (20 μM, 3.6 J/cm^2, L+S+) than those of the control groups including negative control (L-S-), curcumin treatment alone (20 μM, L-S+), and LED irradiation alone (3.6 J/cm^2, L+S-).

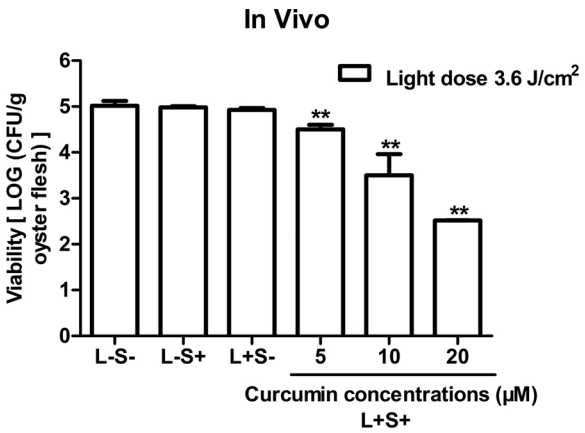

Fig. 4. Viability of DH5α cells in oysters.
L-S-: negative control, contamination with DH5α cells; L-S+: CUR treatment alone, contamination with DH5α cells and 20 μM CUR without irradiation; L+S-: LED irradiation alone, contamination with DH5α cells and irradiation (3.6 J/cm^2); L+S+: CUR-mediated PDI, contamination with DH5α cells and CUR (5, 10 and 20 μM) with irradiation (3.6 J/cm^2). Each column represents the average of triplicates, at least repeated for three times. Values are expressed as mean ± SD. ** $P < 0.01$, different from the L-S- group.

3.4. Inactivation of DH5α contaminated in oysters

After contaminated for 3 h, the oysters accumulated the number of bacteria to a mean value of 5-log (CFU/g oyster flesh) in L-S- group as shown in Fig. 4. The viability of DH5α contaminated in oysters showed that no marked difference ($P > 0.05$) was found between L-S+, L+S- and L-S- groups. CUR-mediated PDI significantly killed DH5α contaminated in oysters. The viability of DH5α reduced significantly ("**" $P < 0.01$) in L+S+ group compared with L-S- group, and the rate of

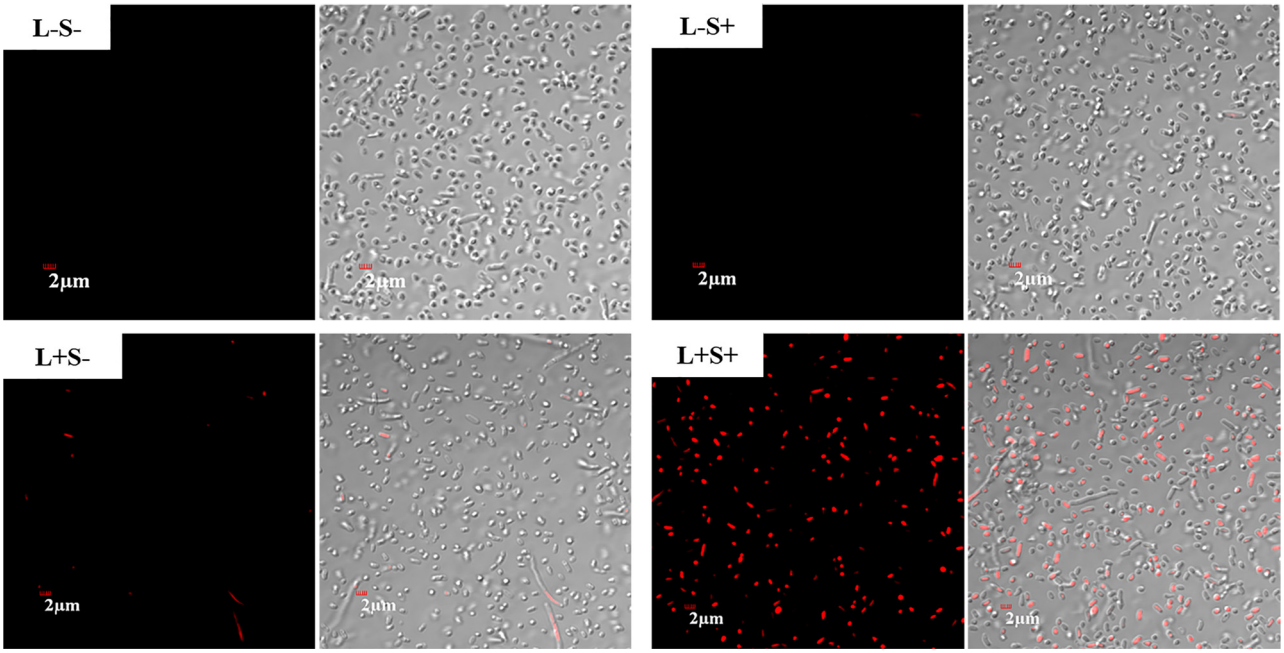

Fig. 3. Membrane permeability of DH5α cells.
Membrane permeability of DH5α cells was measured using CLSM with PI staining. L-S-: negative control; L-S+: CUR treatment alone (20 μM); L+S-: LED irradiation alone (3.6 J/cm^2); L+S+: CUR-mediated PDI (20 μM, 3.6 J/cm^2). It is a representative figure of the final results which were repeated at least for three times.

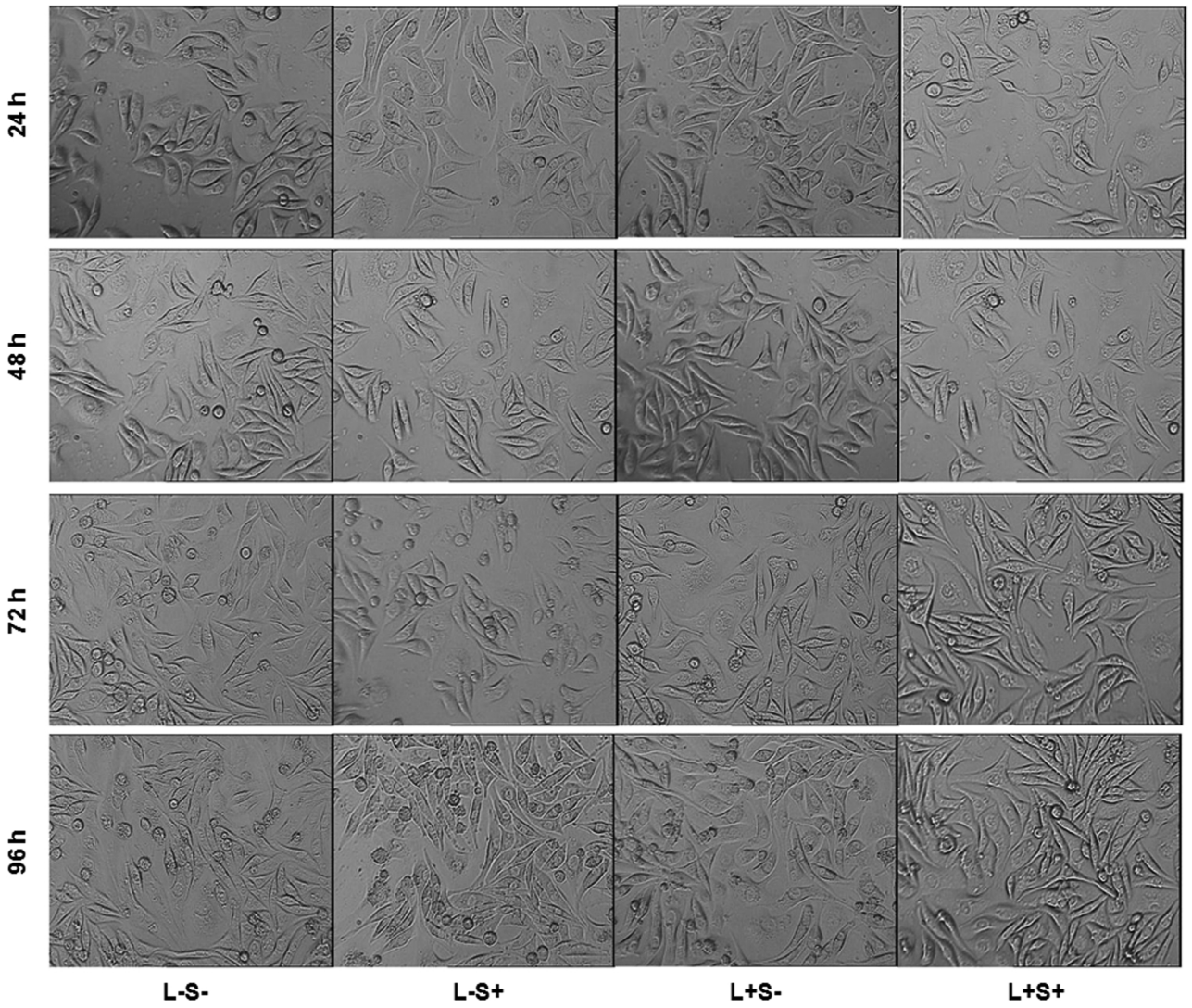

Fig. 5. Morphology changes of L929 cells after incubation with the filtrates of PDI-treated oysters for 24, 48, 72, 96 h (200×).
L-S-: negative control, oysters without treatment; L-S+: CUR treatment alone, oysters incubation with 20 μM CUR without irradiation; L+S-: LED irradiation alone, oysters irradiation (3.6 J/cm^2); L+S+: CUR-mediated PDI, oysters incubation with 20 μM CUR and irradiation (3.6 J/cm^2). It is a representative figure of the final results which were repeated at least for three times.

cell death increased in a CUR concentration-dependent manner and resulted in an approximately 2.5-log (CFU/g oyster flesh) reduction at the concentration of 20 μM. Our results preliminary confirmed that CUR-mediated PDI had an efficient decontamination of DH5α contaminated in oysters.

3.5. Cell morphology changes after incubation with PDI-treated oysters

After incubation with the filtrates of PDI-treated oysters for 24, 48, 72, and 96 h, the morphology of L929 cells was observed using an inverted contrast microscope. As shown in Fig. 5, there was no obvious changes of morphology found in the L+S+ group compared with the other three groups. These findings demonstrated that PDI-treated (20 μM, 3.6 J/cm^2) oysters could not destroy the morphology of L929 cells.

3.6. Cytotoxicity analysis after incubation with PDI-treated oysters

Fig. 6 showed the MTT assay of L929 cells which were incubated with the filtrates of PDI-treated oysters for 24, 48, 72, 96 h respectively. The results of absorbance at 570 nm showed that there was no

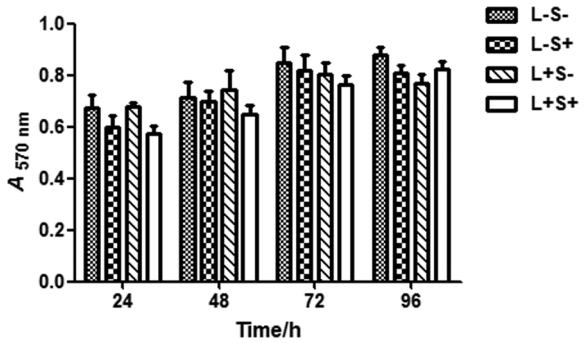

Fig. 6. MTT assay of L929 cells after incubation with the filtrates of PDI-treated oysters for 24, 48, 72, 96 h.
The absorbance at 570 nm was measured using microplate reader. L-S-: negative control, oysters without treatment; L-S+: CUR treatment alone, oysters incubation with 20 μM CUR without irradiation; L+ S-: LED irradiation alone, oysters irradiation (3.6 J/cm^2); L+S+: CUR-mediated PDI, oysters incubation with 20 μM CUR and irradiation (3.6 J/cm^2). Each column represents the average of triplicates, at least repeated for three times. Values are expressed as mean ± SD.

Table 2
Relative growth rates (RGR) and the corresponding cytotoxicity grades.

Groups	24 h		48 h		72 h		96 h	
	RGR	Grade	RGR	Grade	RGR	Grade	RGR	Grade
L-S-	100	0	100	0	100	0	100	0
L-S+	89.2	1	97.6	1	96.1	1	91.8	1
L+S-	100.8	0	104.2	0	94.8	1	87.4	1
L+S+	85.0	1	90.5	1	89.8	1	93.6	1

significant differences ($P > 0.05$) between the L+S+ group and the other three groups. The relative growth rates (RGR) of all the groups were over 85% and the cytotoxicity grades were 0 or 1 (Table 2), indicating no cytotoxicity of PDI-treated (20 μM, 3.6 J/cm^2) oysters to L929 cells.

3.7. Apoptosis analysis after incubation with PDI-treated oysters

DNA ladder assay is a simple, sensitive, cost-effective and rapid method for estimating apoptosis cells. DNA laddering during apoptosis was characterized by agarose gel electrophoresis [41–44]. Apoptosis can be visualized as a ladder pattern of 180–200 bp due to DNA cleavage by the activation of a nuclear endonuclease [45,46]44-45. As shown in Fig. 7, there was no formation of the DNA ladder in gel electrophoresis after incubation with the filtrates of PDI-treated (20 μM, 3.6 J/cm^2) oysters for 96 h.

Induction of apoptosis on L929 cells was also investigated by microscopic analysis of Hoechst 33258 stained cells. L929 cells were stained using Hoechst 33342 96 h after incubation with the filtrates of PDI-treated oysters. Changes of nuclear characteristic in cells were observed under fluorescence microscopy. The results showed that the nuclei of the four groups had no significant changes and the cells were observed a variety of karyomorphism, including round, kidney shape and oval (Fig. 8). These findings demonstrated that PDI-treated (20 μM, 3.6 J/cm^2) oysters did not induce the L929 cell apoptosis. Overall, no cytotoxicity of PDI-treated oysters was found to the fibroblasts according to our current study.

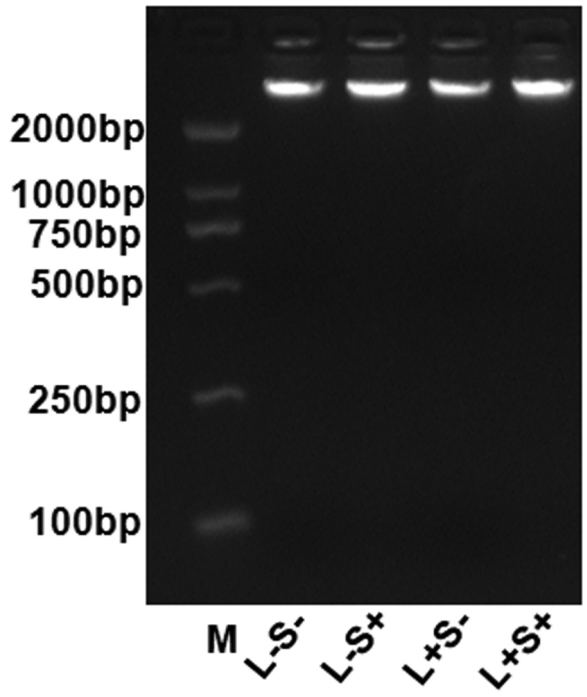

Fig. 7. DNA ladder of L929 cells after incubation with the filtrates of PDI-treated oysters for 96 h.
L929 cells genomic DNA were extracted and separated by 1% agarose gel electrophoresis, stained with ethidium bromide, and visualized using UV light. M: Marker, DL 2000. L-S-: negative control, oysters without treatment; L-S+: CUR treatment alone, oysters incubation with 20 μM CUR without irradiation; L+S-: LED irradiation alone, oysters irradiation (3.6 J/cm^2); L+S+: CUR-mediated PDI, oysters incubation with 20 μM CUR and irradiation (3.6 J/cm^2). It is a representative figure of the final results which were repeated at least for three times.

4. Discussion

Oyster, a kind of bivalve molluscan shellfish, can filter large volumes of water as part of its feeding activities and is able to accumulate and concentrate different types of pathogens, such as *Escherichia Coli*, *Vibrio parahaemolyticus*, *Salmonella*, *Staphylococcus aureus*, *Norovirus*, and so on. According to our previous studies, we found that CUR-mediated PDI could effectively inactivate norovirus and *Vibrio parahaemolyticus* which were contaminated in oysters [3,34]. In the present study, we chosen *Escherichia Coli* DH5α to further explore whether it had a broad-spectrum sterilization efficacy. Our results showed that after treatment with CUR-mediated PDI, the viability of DH5α reduced extremely significant, and the rate of cell death increased in a CUR concentration-dependent manner and resulted in an approximately 3.5-log reduction at the concentration of 20 μM *in vitro*. It also showed a good decontamination effect against DH5α contaminated in oysters with 20 μM CUR under 3.6 J/cm^2 light irradiation. Thus, our findings demonstrated that CUR-mediated PDI had a broad-spectrum antimicrobial activity.

Excessive accumulation of intracellular ROS is a direct or indirect cause of cell death [37]. Excessive ROS can destruct cell membrane, cytoplasmic membrane, and nuclear membrane to directly cause cell death [47–51]. Reports showed that blue light could activate CUR and hypocrellin B to increase the intracellular ROS level in Gram-positive bacteria strain *Staphylococcus aureus* [36,37]. Our results from FCM with DCFH-DA staining also showed the ROS level increased in DH5α cells.

Membrane integrity is a prerequirement of bacterial survival. Our results from CLSM with PI staining observed more red fluorescence in DH5α cells after treatment with CUR-mediated PDI, demonstrating that CUR-mediated PDI increased membrane permeability of the treated DH5α cells. The results were consistent with the research on *Staphylococcus aureus* treated by photodynamic action of CUR [36]. These findings revealed that CUR-mediated PDI damaged membrane permeability probably through the generation of intracellular ROS to eventually cause the DH5α death.

As a food additive, curcumin should be added within the limit standard to guarantee the edible security and reduce the impact on the appearance and flavor of oysters. Our initial data suggest that the appearance and flavor of oysters could be retained after treatment with CUR-mediated PDI [3,34]. Curcumin solution were directly added on cells in cellular toxicological study in our previous study and no cytotoxicity was found. In this article, we extended our previous studies and the filtrates of PDI-treated oysters were used in cytotoxic experiment. After incubation with the filtrates of PDI-treated oysters, the morphology of L929 cells had no obvious changes, RGR was over 85% and cytotoxicity grades were 0 or 1, indicating no cytotoxicity of PDI-treated (20 μM, 3.6 J/cm^2) oysters to L929 cells. DNA ladder and nuclear staining also showed that no apoptosis was found in L929 cells, preliminarily confirmed its edible security from the cellular level, and the further study needs to be conducted from the animal and human levels.

As a natural photosensitizer isolated from the traditional Chinese herbal medicine [23], curcumin and its degradation products are nontoxic and have been studied for diverse biological activities [27–30]. With an irradiation time of 60 s and the energy density of 3.6 J/cm^2, CUR-mediated PDI saves time and energy. In addition, CUR-mediated

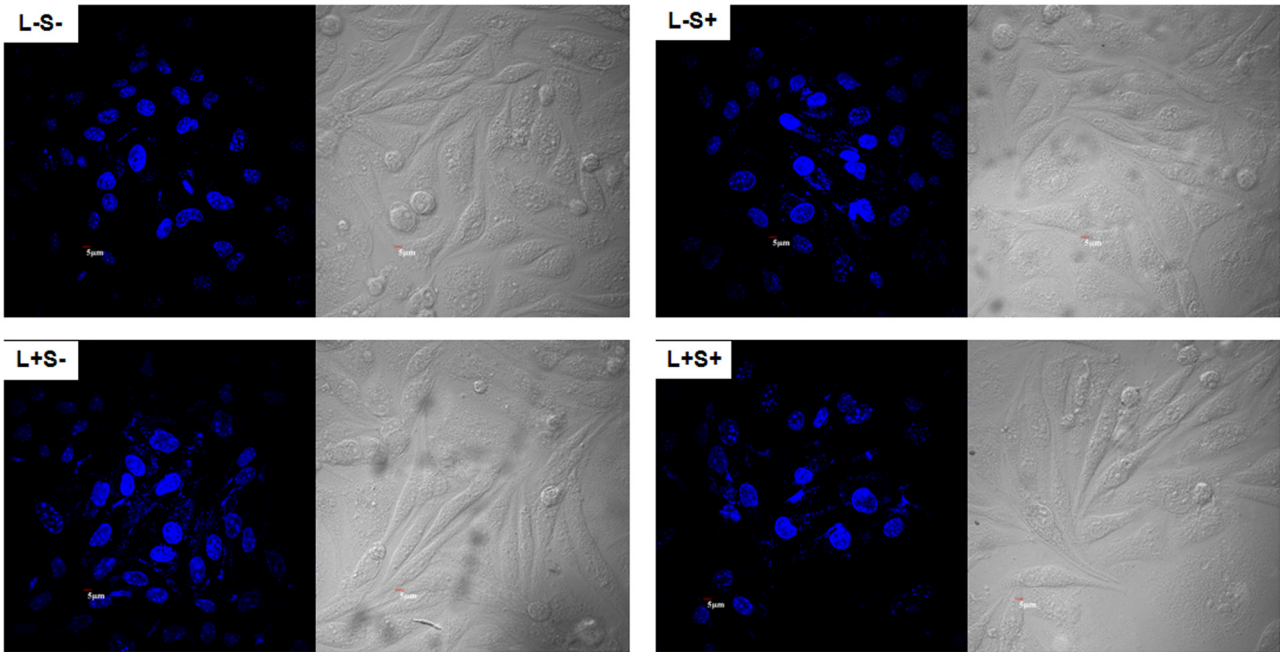

Fig. 8. Nuclear features of L929 cells after incubation with the filtrates of PDI-treated oysters for 96 h.
The nuclei of L929 cells were observed by Hoechst 33258 staining. L-S-: negative control, oysters without treatment; L-S+: CUR treatment alone, oysters incubation with 20 μM CUR without irradiation; L+S-: LED irradiation alone, oysters irradiation (3.6 J/cm^2); L+S+: CUR-mediated PDI, oysters incubation with 20 μM CUR and irradiation (3.6 J/cm^2). Scale bar: 5 μm. It is a representative figure of the final results which were repeated at least for three times.

PDI is effective against a variety of microorganisms and some of them are extremely significant [3,31,33,34,52]. Therefore, the bactericidal effects of CUR-mediated PDI on many kinds of bacteria are widely accepted in the application of food [3,31,33]. CUR-mediated PDI is expected to be developed into a new system for the production and processing of fresh half-shell oysters.

5. Conclusions

This study demonstrated that CUR-mediated PDI could remarkably inactivate DH5α cells both *in vitro* and *in vivo*. The data also highlighted that CUR-mediated PDI could produce intracellular ROS which could cause irreversible damage to the bacteria, leading to bacterial membrane permeability increase and causing the bacterial death eventually. Our data preliminarily confirmed that CUR-mediated PDI-treated oysters had no cytotoxicity to fibroblasts. It is recommended that further studies should be undertaken to explore the edible security of this treated oysters from animal and human levels.

Conflict of interests

The authors declare that they have no competing interests.

Acknowledgments

This work was supported by the National Natural Science Foundation of China [grant number 31871867]; and the Special Fund Project of National Modern Agricultural Industry Technology System of China [grant number CARS-49].

References

[1] W. Burkhardt, K.R. Calci, Selective accumulation may account for shellfish-associated viral illness, Appl. Environ. Microbiol. 66 (2000) 1375–1378, https://doi.org/10.1128/AEM.66.4.1375-1378.2000.
[2] N. Dantas, N. Francis, P. De Oliveira, P. Mirella, Perkinsus infection is associated with alterations in the level of global DNA methylation of gills and gastrointestinal tract of the oyster Crassostrea gasar, J. Invertebr. Pathol. 149 (2017) 76–81, https://doi.org/10.1016/j.jip.2017.08.007.
[3] J. Wu, W. Hou, B. Cao, T. Zuo, C. Xue, A.W. Leung, C. Xu, Q.J. Tang, Virucidal efficacy of treatment with photodynamically activated curcumin on murine norovirus bio-accumulated in oysters, Photodiagnosis Photodyn. Ther. 12 (2015) 385–392, https://doi.org/10.1016/j.pdpdt.2015.06.005.
[4] S.Y. Park, S.C. Bae, S. Do Ha, Heat inactivation of a norovirus surrogate in cell culture lysate, abalone meat, and abalone viscera, Food Environ. Virol. 7 (2014) 58–66, https://doi.org/10.1007/s12560-014-9176-y.
[5] S.-W. Kim, S.-B. Baek, J.-H. Ha, M.H. Lee, C. Choi, S.-D. Ha, Chlorine treatment to inactivate norovirus on food contact surfaces, J. Food Prot. 75 (2012) 184–188, https://doi.org/10.4315/0362-028X.JFP-11-243.
[6] K. Feng, E. Divers, Y. Ma, J. Li, Inactivation of a human norovirus surrogate, human norovirus virus-like particles, and vesicular stomatitis virus by Gamma irradiation, Appl. Environ. Microbiol. 77 (2011) 3507–3517, https://doi.org/10.1128/AEM.00081-11.
[7] D.H. Kingsley, High pressure processing and its application to the challenge of virus-contaminated foods, Food Environ. Virol. 5 (2013) 1–12, https://doi.org/10.1007/s12560-012-9094-9.
[8] Q. Tang, D. Li, J. Xu, J. Wang, Y. Zhao, Z. Li, C. Xue, International Journal of Food Microbiology Mechanism of inactivation of murine norovirus-1 by high pressure processing, Int. J. Food Microbiol. 137 (2010) 186–189, https://doi.org/10.1016/j.ijfoodmicro.2009.10.033.
[9] L. Xiao, T. Tsutsui, N. Miwa, The lipophilic vitamin C derivative, 6-o-palmitoylascorbate, protects human lymphocytes, preferentially over ascorbate, against X-ray-induced DNA damage, lipid peroxidation, and protein carbonylation, Mol. Cell. Biochem. 394 (2014) 247–259, https://doi.org/10.1007/s11010-014-2101-8.
[10] M.Y. Lim, J.M. Kim, G. Ko, Disinfection kinetics of murine norovirus using chlorine and chlorine dioxide, Water Res. 44 (2010) 3243–3251, https://doi.org/10.1016/j.watres.2010.03.003.
[11] M.R. Hamblin, T. Hasan, Photodynamic therapy: A new antimicrobial approach to infectious disease? Photochem. Photobiol. Sci. 3 (2004) 436–450, https://doi.org/10.1039/b311900a.
[12] B. Donnerstag, R.P. Baum, J.B. Oltrogge, K. Henzel, L. Trager, G. Hor, Evaluation of tumor immunity in patients with ovarian cancer after immunoscintigraphy in a long-term follow-up, Hybridoma. 14 (1995) 191–197, https://doi.org/10.1002/lsm.20361.
[13] J. Almeida, J.P.C. Tomé, M.G.P.M.S. Neves, A.C. Tomé, J.A.S. Cavaleiro, Â. Cunha, L. Costa, M.A.F. Faustino, A. Almeida, Photodynamic inactivation of multidrug-resistant bacteria in hospital wastewaters: influence of residual antibiotics, Photochem. Photobiol. Sci. 13 (2014) 626–633, https://doi.org/10.1039/c3pp50195g.
[14] L.N. Dovigo, A.C. Pavarina, E.G. De Oliveira Mima, E.T. Giampaolo, C.E. Vergani, V.S. Bagnato, Fungicidal effect of photodynamic therapy against fluconazole-resistant Candida albicans and Candida glabrata, Mycoses. 54 (2011) 123–130, https://doi.org/10.1111/j.1439-0507.2009.01769.x.
[15] S. Banfi, E. Caruso, L. Buccafurni, V. Battini, S. Zazzaron, P. Barbieri, V. Orlandi, Antibacterial activity of tetraaryl-porphyrin photosensitizers: an in vitro study on Gram negative and Gram positive bacteria, J. Photochem. Photobiol. B, Biol. 85

(2006) 28–38, https://doi.org/10.1016/j.jphotobiol.2006.04.003.
[16] F. Cieplik, A. Pummer, J. Regensburger, K.A. Hiller, A. Späth, L. Tabenski, W. Buchalla, T. Maisch, The impact of absorbed photons on antimicrobial photodynamic efficacy, Front. Microbiol. 6 (2015), https://doi.org/10.3389/fmicb.2015.00706.
[17] L. Costa, J.P.C. Tomé, M.G.P.M.S. Neves, A.C. Tomé, J.A.S. Cavaleiro, Â. Cunha, M.A.F. Faustino, A. Almeida, Susceptibility of non-enveloped DNA- and RNA-type viruses to photodynamic inactivation, Photochem. Photobiol. Sci. 11 (2012) 1520–1523, https://doi.org/10.1039/c2pp25156f.
[18] M.C. Gomes, S.M. Woranovicz-Barreira, M.A.F. Faustino, R. Fernandes, M.G.P.M.S. Neves, A.C. Tomé, N.C.M. Gomes, A. Almeida, J.A.S. Cavaleiro, Â. Cunha, J.P.C. Tomé, Photodynamic inactivation of Penicillium chrysogenum conidia by cationic porphyrins, Photochem. Photobiol. Sci. 10 (2011) 1735–1743, https://doi.org/10.1039/c1pp05174a.
[19] K. Kassab, T. Ben Amor, G. Jori, O. Coppellotti, Photosensitization of Colpoda inflata cysts by meso-substituted cationic porphyrins, Photochem. Photobiol. Sci. 1 (2002) 560–564, https://doi.org/10.1039/b201267g.
[20] J.F. Lovell, T.W.B. Liu, J. Chen, G. Zheng, Activatable photosensitizers for imaging and therapy, Chem. Rev. 110 (2010) 2839–2857, https://doi.org/10.1021/cr900236h.
[21] J. Dougherty, C. Gomer, B. Henderson, G. Jori, D. Kessel, M. Korbelik, J. Moan, Review - photodynamic therapy, J Natl Cancer Inst. (1998).
[22] J. Liao, P.P. Li, C.J. Wu, [Screening new photosensitizers from Chinese medicinal herbs and searching for herbal photodynamic killing effects on human stomach cancer cells], Zhongguo Zhong Xi Yi Jie He Za Zhi 17 (1997) 726–729 http://www.ncbi.nlm.nih.gov/entrez/query.fcgi?cmd=Retrieve&db=PubMed&dopt=Citation&list_uids=10322820.
[23] A.F.M.M. Rahman, R.F. Angawi, A.A. Kadi, Spatial localisation of curcumin and rapid screening of the chemical compositions of turmeric rhizomes (Curcuma longa Linn.) using Direct Analysis in Real Time-Mass Spectrometry (DART-MS), Food Chem. 173 (2015) 489–494, https://doi.org/10.1016/j.foodchem.2014.10.049.
[24] M. Ahmad, S. Akhter, N. Mohsin, B. Abdel-Wahab, J. Ahmad, M. Warsi, M. Rahman, N. Mallick, F. Ahmad, Transformation of curcumin from food additive to multi-functional medicine: nanotechnology bridging the gap, Curr. Drug Discov. Technol. 11 (2014) 197–213, https://doi.org/10.2174/1570163811666140616153436.
[25] R. Hanif, L. Qiao, S.J. Shiff, B. Rigas, Curcumin, a natural plant phenolic food additive, inhibits cell proliferation and induces cell cycle changes in colon adenocarcinoma cell lines by a prostaglandin-independent pathway, J. Lab. Clin. Med. 130 (1997) 576–584, https://doi.org/10.1016/S0022-2143(97)90107-4.
[26] T.R. Arunraj, N.S. Rejinold, S. Mangalathillam, S. Saroj, R. Biswas, R. Jayakumar, Synthesis, characterization and biological activities of curcumin nanospheres, J. Biomed. Nanotechnol. 10 (2014) 238–250, https://doi.org/10.1166/jbn.2014.1786.
[27] S.C. Gupta, S. Patchva, W. Koh, B.B. Aggarwal, Discovery of curcumin, a component of golden spice, and its miraculous biological activities, Clin. Exp. Pharmacol. Physiol. 39 (2012) 283–299, https://doi.org/10.1111/j.1440-1681.2011.05648.x.
[28] A. Meng, G. Gong, D. Chen, H. Zhang, S. Qi, H. Tang, Z. Gao, DNA fingerprint variability within and among parental lines and its correlation with performance of F1 laying hens, Theor. Appl. Genet. 92 (1996) 769–776, https://doi.org/10.1016/j.ejmech.2009.03.020.
[29] R.K. Maheshwari, A.K. Singh, J. Gaddipati, R.C. Srimal, Multiple biological activities of curcumin: a short review, in: Life Sci. (2006) 2081–2087, https://doi.org/10.1016/j.lfs.2005.12.007.
[30] D. Rai, J.K. Singh, N. Roy, D. Panda, Curcumin inhibits FtsZ assembly: an attractive mechanism for its antibacterial activity, Biochem. J. 410 (2008) 147–155, https://doi.org/10.1042/BJ20070891.
[31] R. Tao, F. Zhang, Q. Tang, C. Xu, Z. Ni, X. Meng, Effects of curcumin-based photodynamic treatment on the storage quality of fresh-cut apples, Food Chem. 274 (2019) 415–421, https://doi.org/10.1016/j.foodchem.2018.08.042.
[32] C. Santezi, J.M.G. Tanomaru, V.S. Bagnato, O.B. Oliveira, L.N. Dovigo, Photodiagnosis and Photodynamic Therapy Potential of curcumin-mediated photodynamic inactivation to reduce oral colonization, Photodiagn Photodyn 15 (2016) 46–52.
[33] C. Campos, C. Quishida, E. Garcia, D.O. Mima, J.H. Jorge, C.E. Vergani, V.S. Bagnato, A.C. Pavarina, Photodynamic inactivation of a multispecies biofilm using curcumin and LED light, Lasers Med. Sci. (2016) 997–1009, https://doi.org/10.1007/s10103-016-1942-7.
[34] J. Wu, H. Mou, C. Xue, A.W. Leung, C. Xu, Q.J. Tang, Photodynamic effect of curcumin on Vibrio parahaemolyticus, Photodiagnosis Photodyn. Ther. 15 (2016) 34–39, https://doi.org/10.1016/j.pdpdt.2016.05.004.
[35] V.S. Ghate, K.S. Ng, W. Zhou, H. Yang, G.H. Khoo, W.B. Yoon, H.G. Yuk, Antibacterial effect of light emitting diodes of visible wavelengths on selected foodborne pathogens at different illumination temperatures, Int. J. Food Microbiol. 166 (2013) 399–406, https://doi.org/10.1016/j.ijfoodmicro.2013.07.018.
[36] Y. Jiang, A.W. Leung, H. Hua, X. Rao, C. Xu, Photodynamic action of LED-activated curcumin against staphylococcus aureus involving intracellular ROS increase and membrane damage, Int. J. Photoenergy. 2014 (2014), https://doi.org/10.1155/2014/637601.
[37] Y. Jiang, A.W. Leung, X. Wang, H. Zhang, C. Xu, Inactivation of Staphylococcus aureus by photodynamic action of hypocrellin B, Photodiagnosis Photodyn. Ther. 10 (2013) 600–606, https://doi.org/10.1016/j.pdpdt.2013.06.004.
[38] X. Su, P. Wang, X. Wang, L. Guo, S. Li, Q. Liu, Involvement of MAPK activation and ROS generation in human leukemia U937 cells undergoing apoptosis in response to sonodynamic therapy, Int. J. Radiat. Biol. 89 (2013) 915–927, https://doi.org/10.3109/09553002.2013.817700.
[39] C.H. Kim, C.W. Chung, K.H. Choi, J.J. Yoo, D.H. Kim, Y. Il Jeong, D.H. Kang, Effect of 5-aminolevulinic acid-based photodynamic therapy via reactive oxygen species in human cholangiocarcinoma cells, Int. J. Nanomedicine 6 (2011) 1357–1363, https://doi.org/10.2147/IJN.S21395.
[40] L.C. Crowley, A.P. Scott, B.J. Marfell, J.A. Boughaba, G. Chojnowski, N.J. Waterhouse, Measuring cell death by propidium iodide uptake and flow cytometry, Cold Spring Harb. Protoc. 2016 (2016) 647–651, https://doi.org/10.1101/pdb.prot087163.
[41] C. Lu, F. Zhu, Y.Y. Cho, F. Tang, T. Zykova, W. ya Ma, A.M. Bode, Z. Dong, Cell apoptosis: requirement of H2AX in DNA ladder formation, but not for the activation of Caspase-3, Mol. Cell 23 (2006) 121–132, https://doi.org/10.1016/j.molcel.2006.05.023.
[42] I.K.H. Poon, Y.H. Chiu, A.J. Armstrong, J.M. Kinchen, I.J. Juncadella, D.A. Bayliss, K.S. Ravichandran, Unexpected link between an antibiotic, pannexin channels and apoptosis, Nature. 507 (2014) 329–334, https://doi.org/10.1038/nature13147.
[43] Y.R. Saadat, N. Saeidi, S.Z. Vahed, A. Barzegari, J. Barar, An update to DNA ladder assay for apoptosis detection, Bioimpacts 5 (2015) 25–28, https://doi.org/10.15171/bi.2015.01.
[44] L. Sun, H.Y. Yau, W.Y. Wong, R.A. Li, Y. Huang, X. Yao, Role of trpm2 in H2O2-induced cell apoptosis in endothelial cells, PLoS One 7 (2012), https://doi.org/10.1371/journal.pone.0043186.
[45] Y.A. Ioannou, F.W. Chen, Quantitation of DNA fragmentation in apoptosis, Nucleic Acids Res. 24 (1996) 992–993, https://doi.org/10.1093/nar/24.5.992.
[46] E. Matalová, A. Španová, Detection of apoptotic DNA ladder in pig leukocytes and its precision using LM-PCR (Ligation mediated polymerase chain reaction), Acta Vet. Brno. 71 (2002) 163–168, https://doi.org/10.2754/avb200271020163.
[47] J.C. Ahn, J.W. Kang, J.I. Shin, P.S. Chung, Combination treatment with photodynamic therapy and curcumin induces mitochondria-dependent apoptosis in AMC-HN3 cells, Int. J. Oncol. 41 (2012) 2184–2190, https://doi.org/10.3892/ijo.2012.1661.
[48] L. Huang, Y. Xuan, Y. Koide, T. Zhiyentayev, M. Tanaka, M.R. Hamblin, Type i and Type II mechanisms of antimicrobial photodynamic therapy: an in vitro study on gram-negative and gram-positive bacteria, Lasers Surg. Med. 44 (2012) 490–499, https://doi.org/10.1002/lsm.22045.
[49] C.S. Lunde, S.R. Hartouni, J.W. Janc, M. Mammen, P.P. Humphrey, B.M. Benton, Telavancin disrupts the functional integrity of the bacterial membrane through targeted interaction with the cell wall precursor lipid II, Antimicrob. Agents Chemother. 53 (2009) 3375–3383, https://doi.org/10.1128/AAC.01710-08.
[50] T. Maisch, J. Baier, B. Franz, M. Maier, M. Landthaler, R.-M. Szeimies, W. Baumler, The role of singlet oxygen and oxygen concentration in photodynamic inactivation of bacteria, Proc. Natl. Acad. Sci. 104 (2007) 7223–7228, https://doi.org/10.1073/pnas.0611328104.
[51] U.S. Dwivedi, N.K. Goyal, V. Saxena, R.L. Acharya, S. Trivedi, P.B. Singh, N. Vyas, B. Datta, A. Kumar, S. Das, Xanthogranulomatous pyelonephritis: our experience with review of published reports, ANZ J. Surg. 76 (2006) 1007–1009, https://doi.org/10.1111/j.1445-2197.2006.03919.x.
[52] A.C. Pavarina, L.N. Dovigo, C.E. Vergani, V.S. Bagnato, J.C. Carmello, I.L. Brunetti, C.A. de Souza, Costa, Curcumin-mediated photodynamic inactivation of Candida albicans in a murine model of oral candidiasis, Med. Mycol. 51 (2012) 243–251, https://doi.org/10.3109/13693786.2012.714081.